Published in final edited form as:
IEEE Trans Biomed Eng. 2008 October ; 55(10): 2444–2451. doi:10.1109/TBME.2008.925700.

Electromagnetic Spectroscopy of Normal Breast Tissue Specimens Obtained From Reduction Surgeries: Comparison of Optical and Microwave Properties

Mariya Lazebnik [Student Member, IEEE],
Department of Electrical and Computer Engineering, University of Wisconsin-Madison, Madison, WI 53706 USA

Changfang Zhu [Student Member, IEEE],
Department of Electrical and Computer Engineering, University of Wisconsin-Madison, Madison, WI 53706 USA

Gregory M. Palmer,
Department of Biomedical Engineering, Duke University, Raleigh, NC 27708 USA

Josephine Harter,
Department of Pathology, University of Wisconsin-Madison, Madison, WI 53706 USA

Sarah Sewall,
Department of Pathology, University of Wisconsin-Madison, Madison, WI 53706 USA

Nirmala Ramanujam, and
Department of Biomedical Engineering, Duke University, Raleigh, NC 27708 USA

Susan C. Hagness [Senior Member, IEEE]
Department of Electrical and Computer Engineering, University of Wisconsin-Madison, Madison, WI 53706 USA

Mariya Lazebnik: mariya.lazebnik@gmail.com; Changfang Zhu: nimmi@duke.edu; Gregory M. Palmer: ; Josephine Harter: ; Sarah Sewall: ; Nirmala Ramanujam: ; Susan C. Hagness: hagness@engr.wisc.edu

Abstract

Techniques utilizing electromagnetic energy at microwave and optical frequencies have been shown to be promising for breast cancer detection and diagnosis. Since different biophysical mechanisms are exploited at these frequencies to discriminate between healthy and diseased tissue, combining these two modalities may result in a more powerful approach for breast cancer detection and diagnosis. Toward this end, we performed microwave dielectric spectroscopy and optical diffuse reflectance spectroscopy measurements at the same sites on freshly-excised normal breast tissues obtained from reduction surgeries at the University of Wisconsin Hospital, using microwave and optical probes with very similar sensing volumes. We found that the microwave dielectric constant and effective conductivity are correlated with tissue composition across the entire measurement frequency range ($|r|$~0.5–0.6, $p<0.01$), and that the optical absorption coefficient at 460 nm and optical scattering coefficient are correlated with tissue composition ($|r|$~ 0.4–0.6, $p<0.02$). Finally, we found that the optical absorption coefficient at 460 nm is correlated with the microwave dielectric constant and effective conductivity ($r=-0.55$, $p<0.01$). Our results suggest that combining optical and microwave modalities for analyzing breast tissue samples may serve as a crosscheck and provide complementary information about tissue composition.

Index Terms

Breast cancer detection; breast cancer diagnosis; breast tissue; dielectric spectroscopy; diffuse reflectance spectroscopy; microwave measurements; optical measurements

I. INTRODUCTION

Although x-ray mammography and open surgical biopsy are currently the gold standards for breast cancer detection and diagnosis, respectively, neither approach is ideal. Mammography suffers from high false-negative and false-positive rates [1], [2]. In addition, mammography utilizes high-frequency ionizing radiation and requires uncomfortable breast compression, which can discourage women from seeking regular exams that are necessary for timely detection of potential malignancies. Open surgical biopsy is performed in the operating room and requires general anesthesia. Needle biopsy, a minimally invasive alternative, is less expensive, faster, and requires a shorter recovery time. However, the sampling accuracy of needle biopsy is limited because only a few small pieces of tissue are sampled from the suspicious mass. Consequently, this procedure has a false-negative rate of 1%–7% when verified with follow up mammography [3], and repeat biopsies are required in 9%–18% of patients due to discordance between histological findings and mammography [4], [5].

Screening and diagnostic techniques that employ electromagnetic signals at microwave or optical frequencies aim to overcome some of the above-stated challenges. For example, a number of research groups are currently investigating electromagnetic breast cancer detection techniques in the microwave frequency range [6]–[13]. These low-cost, noninvasive techniques illuminate the breast with extremely low-power, non-ionizing microwave signals and create images from the microwave scattered signals. As another example, diffuse reflectance spectroscopy is being investigated as a tool for characterizing tissue pathology [14]–[16]. This technology is cost-effective, and can be deployed through fiber-optic probes to quickly, non-destructively and quantitatively characterize tissue pathology *in vivo*. The physical basis for the aforementioned techniques is the predicted sensitivity of electromagnetic properties at both microwave and optical frequencies to the tissue's physiological state (see, for example [17]).

At microwave frequencies, the polarization response of the tissue is quantified via the frequency-dependent complex dielectric constant, $\hat{\varepsilon}(\omega)$. At optical wavelengths, diffuse reflectance spectroscopy provides a measure of absorption (quantified via the absorption coefficient, μ_a and scattering (quantified via the reduced scattering coefficient, μ_s') properties of tissue. Since different biophysical mechanisms are at play in the optical and microwave regions of the electromagnetic spectrum, more effective detection and diagnosis may be achieved by combining microwave and optical sensing modalities. In fact, Poplack *et al* [18] showed that multimodality breast imaging that combines three electromagnetic techniques – near-infrared spectroscopy, electrical impedance spectroscopy, and microwave imaging spectroscopy – may enhance detectability of abnormalities over each individual imaging technique.

Lazebnik *et al* [19], [20] recently reported the results of a large-scale study of the microwave properties of normal and malignant breast tissue samples obtained from breast reduction and cancer surgeries at the University of Wisconsin and University of Calgary. Zhu *et al* [21], [22] also recently reported the results of an analogous study of the optical properties of breast tissue samples obtained from surgeries at the University of Wisconsin. The tissue composition of the characterized samples was carefully analyzed and correlated with the measured properties. In both frequency regimes, the electromagnetic properties were shown to be

sensitive to the specific tissue composition. These promising findings motivate the next step involving a comparison of the microwave and optical properties of breast tissue to determine the extent to which the properties are correlated. The logical starting point for this next step is a basic-science study of normal breast tissue, as it establishes a foundation for future studies on diseased tissue.

In this paper, we compare and correlate the microwave and optical properties of a variety of normal breast tissue samples with *known* tissue composition. The data sets that we use in this study were subsets of the large-scale studies reported in [19], [22]. The subset included those normal samples obtained from reduction surgeries for which the microwave and optical measurements were conducted at the same sites within minutes of each other using probes that have very similar sensing volumes.

This work addresses an important gap in the scientific literature, as very little data has been published to date correlating the optical and microwave properties of normal breast tissue. To the best of our knowledge, the only previous study on this topic was published by Poplack *et al* [23]. The average tissue property values at microwave and optical frequencies were compared in 23 negative-diagnosis women undergoing screening mammography. The properties were obtained by imaging the patients breasts using three non-invasive electromagnetic modalities - near-infrared spectroscopy, electrical impedance spectroscopy, and microwave imaging spectroscopy. However, since the study involved *in vivo* imaging, and no histological analysis was performed, the actual composition of the breast tissue was not known precisely. Instead, body mass index (BMI) was used as an indirect measure of breast adipose tissue content.

The remainder of this paper is organized as follows. Section II describes the tissue collection and handling protocol, as well as the data acquisition, processing, and analysis methods. Section III presents the microwave and optical spectroscopy results, as well as correlations between microwave and optical data. In addition, we present a comparison between the results of this study and previously published work. Finally, Section IV summarizes the conclusions of this work.

II. EXPERIMENTAL PROCEDURES

A. Source of tissue samples

We obtained 60 normal breast tissue specimens from 17 patients undergoing breast reduction surgeries at the University of Wisconsin Hospital and Clinics. Patient age ranged between 21 and 64 years. The tissue handling protocol will be briefly summarized here; see [19] for a more detailed description. The freshly excised tissue specimens were transported to the measurement site (the pathology suite at the hospital) within 80 minutes of excision in heated, sealed, and insulated containers to minimize desiccation. Specimen size ranged from approximately 2×2 cm^2 to 10×10 cm^2, and specimen thickness was always at least 4 mm. The optical spectroscopy measurements were conducted no more than one to two minutes following the microwave spectroscopy measurements.

We aimed to take a measurement on a sample of adipose and a sample of fibroconnective/glandular tissue from the right and left breasts of each patient. However, in the case of some patients, we were unable to collect all four measurements for reasons such as inadequate specimen size. The database of measurements analyzed in this study are subsets of the larger databases analyzed in [19], [22].

B. Data acquisition

a) Microwave dielectric spectroscopy—Microwave-frequency dielectric spectroscopy was conducted from 0.5 to 20 GHz using a precision open-ended coaxial probe connected to a vector network analyzer. The 3-mm-diameter flange-free precision probe is very well-suited for this application because 1) the small diameter allows for excellent contact with the tissue sample across the entire probe aperture, 2) the hermetically-sealed aperture prevents fluid leakage into the aperture, and 3) the materials are chemically stable and thermally matched, allowing for long-term robustness and stability of the probe performance. The dielectric measurement procedure used in these experiments was previously described in detail elsewhere [24], and will be summarized here. The complex reflection coefficient at the calibration plane of the open-ended coaxial probe was recorded. A de-embedding model, based on probe-specific numerical simulations that took into account the specific probe geometry, was used to translate the reflection coefficient from the calibration plane to the aperture plane. Then, a rational function model originally proposed in [25], [26] and adapted for our probe in [24] was used to convert the aperture plane reflection coefficient to the frequency-dependent complex permittivity of the sample under test:

$$\hat{\varepsilon}(\omega)=\varepsilon_r(\omega) - j\sigma(\omega)/(\omega\varepsilon_0),$$

where ω is the radial frequency, $j=\sqrt{-1}$, ε_r is the dielectric constant, σ is the effective conductivity, and ε_0 is the permittivity of free space.

b) Optical spectroscopy—Diffuse reflectance spectra of breast tissues were measured over the wavelength range of 350–600 nm using a fiber optic probe coupled to a multi-wavelength optical spectrometer. The spectrometer and instrument parameters have been described in detail elsewhere [27]. The common end of the fiber-optic probe (which is in contact with the tissue) has a central illumination core and three concentric rings of collection fibers surrounding the central core. In this study, only the diffuse reflectance spectra measured with the inner collection ring was analyzed, to ensure that the breast tissue samples could be modeled as a semi-infinite medium over the wavelength range and for the range of sample thickness examined in this study; the outer collection rings which have greater optical sensing depths were excluded [21], [22]. A Monte Carlo based inverse model developed previously [28] was employed to extract the absorption and scattering properties of breast tissues from the measured diffuse reflectance spectra. The outputs from the inverse Monte Carlo model include the size and density of scatterers, the concentrations of oxygenated and deoxygenated hemoglobin, and β-carotene, which are the primary light absorbers in the visible spectral range that are presumed to be present in breast tissue. Absorption and reduced scattering coefficients were calculated from these extracted parameters for the wavelength range of 350–600 nm.

The absorption coefficients were calculated using the extracted concentration of each absorber and their wavelength-dependent extinction coefficients. In this study, we analyzed absorption coefficients at specific wavelengths: 420 nm, a Soret band of hemoglobin absorption; 460 nm, a peak absorption band of β-carotene; and 540 nm and 575 nm, which are α and β peaks of hemoglobin absorption [29]. Reduced scattering coefficients were calculated from the scatterer size, density, and refractive index mismatch between the scatterer and surrounding medium using Mie theory for spherical particles [30]. The reduced scattering coefficient was used rather than the scatterer size or density because different values of scatterer diameter and density can yield similar values for the reduced scattering coefficient using Mie theory. Thus, the reduced scattering coefficient, which directly affects the diffuse reflectance spectra, was used to describe the scattering property. Also, the reduced scattering coefficients were averaged over

the wavelength range to obtain the mean reduced scattering coefficient, in order to be consistent with the way the scattering properties of human tissues are reported in the literature.

c) Microwave and optical probe sensing volumes—The sensing depth of the microwave dielectric probe was previously determined to be ~1.25–3 mm, which is a function of the dielectric constant of the material under test [31]. Although these values are useful guidelines, we note that the measured dielectric properties are heavily influenced by the tissue directly beneath the probe aperture. The diffuse reflectance sensing depth of the multiseparation probe was evaluated using Monte Carlo simulations, and found to be approximately 0.5–2 mm [32]. Since the sensing depths of the microwave and optical probes are very similar, the comparison between the microwave and optical properties extracted from the measurements is justified.

d) Histological analysis—Immediately following each measurement, we marked the exact probe placement site on each tissue specimen using black ink, and a medial cross-sectional slice was cut and processed to create a histological slide (see diagram in Fig. 1). A microscope was used to create a digital image of a 5 mm depth by 7 mm crosswise region of the slide. Subsequently, a pathologist conducted a histological analysis of each slide. The tissue composition in the sensing volume of the probes was broadly categorized in terms of percentages of adipose, glandular, dense fibrous, and loose connective tissues. We combined the dense fibrous and loose connective tissue type categories into a single “fibroconnective” tissue type.

C. Method of data analysis

We applied the exclusionary criteria reported in [19], to minimize uncertainty in the determination of tissue composition within the probes’ sensing volumes, and to ensure consistency of the collected microwave spectroscopy data with the Kramers-Kronig relation [19]. Based on these criteria, we excluded 28 samples, leaving 32 samples for final analysis. Of these, three samples contained 0–30% adipose tissue content, 11 samples contained 31–84% adipose tissue content, and 18 samples contained 85–100% adipose tissue content. To calculate correlations between the various parameters, we used the Spearman rank correlation, instead of the more common Pearson correlation. The latter is a parametric method, which assumes that both data sets are sampled from populations that have, at least approximately, a normal (Gaussian) distribution. The Spearman rank correlation, a non-parametric method, is a good alternative when population sizes are small and a normal distribution cannot be assumed. Its calculation is based on ranking the two variables and makes no assumption about the distributions. We calculated the correlation coefficients (r) between the data sets using the MATLAB function *corr*. Finally, we fit a line to the data using the MATLAB function *polyfit* in order to visually demonstrate the correlations between the various parameters under consideration.

III. RESULTS AND DISCUSSION

In this section, we first present an overview of the results of the statistical analysis, followed by a detailed discussion of the correlations between microwave parameters (ε_r and σ) and tissue composition, correlations between optical parameters (μ_a and μ_s') and tissue composition, and correlations between microwave and optical parameters. We also compare the results of our study with previously published work.

A. Overview

Table I summarizes the results of the correlations between tissue composition and microwave properties (dielectric constant and effective conductivity) at 5, 10, and 15 GHz. These three

frequencies were chosen as representative points across the wide frequency range of our measurements. Similarly, Table II summarizes the correlations between tissue composition and optical properties (mean reduced scattering coefficient and absorption coefficient) at 420, 460, 540 and 575 nm. Finally, Table III summarizes the correlations between the dielectric constant and effective conductivity at 5, 10, and 15 GHz and the mean reduced scattering coefficient and absorption coefficients at 460 nm, 540 nm, and 575 nm. In all tables, the absence of a statistically significant correlation is indicated by a zero (0). Correlations were considered statistically significant for $p<0.01$.

Fig. 2 shows the dielectric constant and effective conductivity at 10 GHz as a function of the absorption coefficient at 460 nm. The circles represent the data points, while the straight lines are fits to the data points. The correlation coefficients and *p*-values are shown in the boxes in the figures.

B. Microwave correlations

We found statistically significant, though moderate ($|r|\sim0.5–0.6$, $p<0.01$), correlations between the microwave dielectric properties and breast tissue composition (see Table I). The correlation coefficients at 5, 10, and 15 GHz are very similar, indicating that these parameters are correlated across the entire measurement frequency range. Both the dielectric constant and effective conductivity tend to decrease as the adipose content of a tissue sample increases. Conversely, as the percent glandular and/or fibroconnective tissue increases, both the dielectric constant and effective conductivity increase. These trends most likely arise due to the large differences in water content of adipose and other tissue types [33]. As the adipose content in a particular tissue sample increases, the water content is reduced, corresponding to the reduced microwave dielectric properties. These results are consistent with general understanding of dielectric spectroscopy of biological tissues [34], [35], as well as the findings reported in [19] for the larger dataset, indicating that the reduced number of samples analyzed here did not skew the dielectric properties results.

C. Optical correlations

We found statistically significant, though moderate ($|r|\sim0.4–0.6$, $p<0.02$), correlations between the optical properties and breast tissue composition (see Table II). The absorption coefficients at 420, 540 and 575 nm do not show statistically significant correlation with tissue properties. The mean reduced scattering coefficient decreases, while the absorption coefficient at 460 nm increases, as the adipose content of the tissue samples increases. This result agrees with expectation because 460 nm is the peak absorption band of β-carotene, which is a carotenoid and an optically active absorber primarily stored in adipose tissue. The mean reduced scattering coefficient increases, while the absorption coefficient at 460 nm decreases, as the glandular and fibroconnective contents of the tissue samples increase. These results are consistent with the results from the larger database analyzed in [22], indicating that the results are not skewed by the smaller number of samples analyzed in this study.

D. Microwave-optical cross-correlations

We found statistically significant, though moderate ($r=-0.55$, $p<0.01$), correlations between the optical absorption coefficient at 460 nm and the microwave dielectric properties across the entire measurement frequency range (see Table III and Fig. 2). This correlation agrees with expectation, since the absorption coefficient and dielectric properties are influenced to a large extent by the quantity of adipose tissue in a particular tissue sample.

We did not find a correlation between the microwave dielectric properties and any other optical parameters analyzed in this study. The fact that we found no correlation between the mean reduced scattering coefficient and the microwave dielectric properties is surprising given that

both the dielectric constant and effective conductivity are correlated with tissue composition, and the mean reduced scattering coefficient is correlated with tissue composition. One possible explanation for this finding is that the correlation between the mean reduced scattering coefficient and glandular tissue content is not as strong ($p<0.02$) as the correlation between the dielectric constant and effective conductivity and the glandular tissue content ($p<0.01$).

E. Comparison with previous studies

1) Microwave correlations—We compared our data for samples with 95% and greater adipose content (16 samples) with the infiltrated fat data reported by Gabriel *et al* [36] at 10 GHz, as well as adipose tissue data reported by Campbell and Land [37] at 3.2 GHz. In the former study, no quantitative tissue composition of "infiltrated fat" was provided; in the latter study, the water content of adipose tissue ranged from 11 to 31% by weight. In our study, the average dielectric constant of samples with 95% or greater adipose content at 10 GHz was 8.7, and the average effective conductivity was 1.7 S/m. The properties reported in [36] at this frequency ranged from about 3 to 10 for dielectric constant, and about 0.2 S/m to 2 S/m for effective conductivity, which agrees very well with our data. The average dielectric constant of the samples measured in our study at 3.2 GHz was approximately 10.6, and the average effective conductivity was approximately 0.41 S/m. Campbell and Land [37] reported the dielectric constant of adipose tissue at this frequency ranging between 2.8 and 7.6, and the effective conductivity ranging between 0.054 S/m and 0.29 S/m, which is slightly lower than the values found in our study. We believe this may be due to differences between in the measurement protocol. The extra handling required for inserting the tissue samples into a resonant cavity [37] may have led to fluid loss from the tissue samples, resulting in slightly reduced microwave-frequency dielectric properties.

Poplack *et al* [23] found a moderate negative correlation between the microwave properties and BMI, although not to statistically significant levels. We suspect that this may be due to the fact that BMI is not a direct measure of adipose tissue content in the breast.

2) Optical correlations—Peters *et al* [38] reported the absorption and reduced scattering coefficients at 540 nm for *ex vivo* normal adipose breast tissue to be approximately 2.3 cm^{-1} and 10.3 cm^{-1}, respectively. In the study by Ghosh *et al* [15], the average absorption and reduced scattering coefficients for normal breast tissues (which were primarily adipose) ranged from approximately 1 to 1.5 cm^{-1} and from approximately 16.4 to 22 cm^{-1}, respectively, within the 450–600 nm wavelength range. Our estimate of the average absorption coefficients for breast samples containing 95% or greater adipose tissue content ranged from 1.02 to 7.75 cm^{-1}, and the average reduced scattering coefficients ranged from 13.7 to 17.9 cm^{-1} within the 450 – 600 nm spectral range. At 540 nm in particular, the average absorption and reduced scattering coefficients of the samples with 95% or greater adipose tissue content were 1.93 cm^{-1} and 14.95 cm^{-1}, respectively. The values of our estimates of μ_a and μ_s' were close to those of Peters *et al* [38] and Ghosh *et al* [15].

The lack of statistically significant correlation between absorption coefficients at 420, 540 and 575 nm and tissue composition in our study implies that no important correlation was observed between the total hemoglobin content and tissue composition. This conclusion differs from those of Durduran *et al* [39], Poplack *et al* [23], and Spinelli *et al* [40], who found that the total hemoglobin content decreased when BMI increased. We believe that this discrepancy is due to several factors: 1) their observations were based on the optical properties of bulk breast tissues and were conducted in the near-infrared spectral range, while in our study, the tissue volumes were more localized, and the wavelengths interrogated were in the UV-Vis spectral range, 2) we measured freshly-excised breast tissue samples, whereby the surgical and pathological dissections may have resulted in blood drainage from the cut surface, affecting

the actual contributions of hemoglobin to the optical measurements [41], and 3) we used adipose content estimated from the histological section as a measure of tissue composition, while previous studies used BMI as a measure of tissue composition.

Our finding that the reduced scattering coefficient is inversely related to the adipose tissue content agrees with the findings from previously published studies. For example, Cerussi *et al* [42] showed that the scattering power decreased with increasing BMI, and Durduran [39] reported that scattering coefficient decreased with BMI.

3) Microwave-optical cross-correlations—Poplack *et al* [23] found a strong correlation (r=0.80) between microwave conductivity and total hemoglobin concentration at near-infrared response (NIR) spectroscopy, suggesting that it is sensitive to local blood volume increases in tissues. However, we did not find a similar result. Again, this discrepancy may be due to the difference in measurement methodology between our study and that of [23].

F. Correlations between microwave parameters and patient age, and optical parameters and patient age

We found no statistically significant correlation between patient age and microwave dielectric properties, and no statistically significant correlation between patient age and optical properties. Poplack *et al* [23] found a small (2–11%) decrease in the dielectric properties at 600 MHz with increasing patient age, though not to statistically significant levels. We did not expect to observe a correlation between microwave properties and patient age since very small tissue volumes, specifically selected for their tissue compositions, were analyzed in our study. Therefore, even though the adipose content of bulk breast tissue may increase as a woman ages (which may be confirmed by Poplack *et al* [23]), this effect would not be evident in our study since we are not analyzing bulk breast tissue specimens. These results are also consistent with the conclusions of the large-scale study reported by Lazebnik *et al* [19]. In addition, we did not observe a correlation of the mean reduced scattering coefficient, or the absorption coefficient at 460 nm, with patient age, which agrees with the conclusions of Cerussi *et al* [42] and Durduran *et al* [39].

G. Implications

In this study, we correlated the microwave and optical properties of normal breast tissue samples with known tissue composition. We did not report analogous correlations for malignant tissues, since the number of malignant samples obtained from cancer surgeries that were simultaneously characterized using microwave and optical techniques was too small to perform reliable statistical analyses. Nevertheless, the microwave and optical properties of malignant breast tissues have been independently previously published in [20] and [21]. We believe that the direct comparisons between microwave and optical properties of normal breast tissues reported here, coupled with the independent reports of microwave and optical properties of malignant breast tissue in [20] and [21], establishes a scientific foundation for future work involving the development of a multi-modality approach for enhancing breast tissue characterization and ultimately breast cancer diagnosis. One example of such a joint modality is a non-invasive electromagnetic imaging approach that combines microwave and NIR techniques (see [18], [23]). A second example is a multi-modality probe used during core needle biopsies for real-time *in situ* diagnosis of potential abnormalities, as well as intra-operative assessment of breast tumor margins.

IV. CONCLUSIONS

In this paper, we reported the results of our investigation to compare and correlate the optical and microwave properties of normal breast tissue samples with known tissue compositions

obtained from reduction surgeries at the University of Wisconsin Hospital and Clinics. The dielectric and optical spectroscopy measurements were conducted at the same sites on freshly excised tissue samples within minutes of each other, utilizing probes with very similar sensing volumes. Since the microwave and optical techniques characterize different physical properties of the tissue samples – β-carotene concentration and cell structural properties at optical frequencies, and water content at microwave frequencies – a multi-modality technique may be able to provide a more comprehensive assessment of tissue histology.

We found that moderate statistically significant correlations exist between microwave properties and tissue composition. Moderate statistically significant correlations were found between optical properties and tissue composition. No statistically significant correlations were found between microwave properties and patient age, and optical properties and patient age. Most importantly, we demonstrated moderate statistically significant correlations between microwave dielectric properties and the optical absorption coefficient at 460 nm, and no statistically significant correlations between microwave properties and the other optical properties. The correlated parameters may be useful as a crosscheck of microwave and optical modalities, while the uncorrelated properties may provide complementary information about tissue composition.

Acknowledgments

The authors would like to thank the following individuals at the University of Wisconsin Hospital for their assistance with and support of this work: Dr. Michael Bentz, Dr. David Dibbell, Jeffrey Fenne, Dr. Kennedy Gilchrist, Dr. Karol Gutowski, Dr. Frederick Kelcz, Debra Martin, Dr. Delora Mount, Deb O'Malley, and Dr. Venkat Rao. In addition, we would like to thank Dr. Mark Converse, Dina Hagl, and Kaitlyn Booske for their assistance with several of the measurements and some of the data processing.

This work was supported by the National Institutes of Health under grant R01CA87007 and the National Science Foundation under a Graduate Research Fellowship.

REFERENCES

1. Elmore JG, Barton MB, Moceri VM, Polk S, Arena PJ, Fletcher SW. Ten-year risk of false positive screening mammograms and clinical breast examinations. New England Journal of Medicine 1998;vol. 338(16):1089–1096. [PubMed: 9545356]
2. Huynh PT, Jarolimek AM, Daye S. The false-negative mammogram. Radiographics 1998;vol. 18(5): 1137–1154. [PubMed: 9747612]
3. Jackman RJ, Nowels KW, Rodriguez-Soto J, M FA Jr, Finkelstein SI, Shepard MJ. Stereotactic, automated, large-core needle biopsy of nonpalpable breast lesions: False-negative and histologic underestimation rates after long-term follow-up. Radiology 1999;vol. 210:799–805. [PubMed: 10207484]
4. Dershaw DD, Morris EA, Liberman L, Abramson AF. Nondiagnostic stereotaxic core breast biopsy: Results of rebiopsy. Radiology 1996;vol. 198:323–325. [PubMed: 8596825]
5. Meyer JE, Smith DN, Lester SC, DiPiro PJ, Denison CM, Harvey SC, Christian RL, Richardson A, Ko WD. Large-needle core biopsy: Nonmalignant breast abnormalities evaluated with surgical excision or repeat core biopsy. Radiology 1998;vol. 206:717–720. [PubMed: 9494490]
6. Meaney PM, Fanning MW, Li D, Poplack S, Paulsen KD. A clinical prototype for active microwave imaging of the breast. IEEE Trans. Micr. Theory Tech 2000 Nov;vol. 48(11):1841–1853.
7. Fear EC, Li X, Hagness SC, Stuchly MA. Confocal microwave imaging for breast cancer detection: Localization of tumors in three dimensions. IEEE Trans. Biomed. Eng 2002 August;vol. 49(8):812–822. [PubMed: 12148820]
8. Bond EJ, Li X, Hagness SC, Veen BDV. Microwave imaging via space-time beamforming for early detection of breast cancer. IEEE Trans. Ant. Prop 2003 August;vol. 51(8):1–16.

9. Zhang ZQ, Liu QH, Xiao C, Ward E, Ybarra G, Joines WT. Microwave breast imaging: 3D forward scattering simulation. IEEE Trans. Biomed. Eng 2003 October;vol. 50(10):1180–1189. [PubMed: 14560772]
10. Li X, Davis SK, Hagness SC, van der Weide DW, Veen BDV. Microwave imaging via space-time beamforming: Experimental investigation of tumor detection in multilayer breast phantoms. IEEE Trans. Micr. Theory Tech 2004 August;vol. 52(8):1856–1865.
11. Kosmas P, Rappaport C. FDTD-based time reversal for microwave breast cancer detection - Localization in three dimensions. IEEE Trans. Micr. Theory Tech 2006;vol. 54:1921–1927.
12. Winters DW, Bond EJ, Veen BDV, Hagness SC. Estimation of the frequency-dependent average dielectric properties of breast tissue using a time-domain inverse scattering technique. IEEE Trans. Ant. Prop 2006;vol. 54:3517–3528.
13. Meaney PM, Fanning MW, Raynolds T, Fox CJ, Fang QQ, Kogel CA, Poplack SP, Paulsen KD. Initial clinical experience with microwave breast imaging in women with normal mammography. Academic Radiology 2007;vol. 14:207–218. [PubMed: 17236994]
14. Bigio IJ, Mourant JR. Ultraviolet and visible spectroscopies for tissue diagnostics: fluorescence spectroscopy and elastic-scattering spectroscopy. Phys. Med. Biol 1997;vol. 42:803–814. [PubMed: 9172260]
15. Ghosh N, Mohanty SK, Majumder SK, Gupta PK. Measurement of optical transport properties of normal and malignant human breast tissue. Appl. Optics 2001;vol. 40:176–184.
16. Zonios G, Perelman LT, Backman V, Manoharan R, Fitzmaurice M, Dam JV, Feld MS. Diffuse reflectance spectroscopy of human adenomatous colon polyps in vivo. Appl. Opt 1999;vol. 38:6628–6637. [PubMed: 18324198]
17. Foster KR, Schwan HP. Dielectric properties of tissues and biological materials: A critical review. Crit. Rev. Biomed. Eng 1989;vol. 17:25–104. [PubMed: 2651001]
18. Poplack SP, Tosteson TD, Wells WA, Pogue BW, Meaney PM, Hartov A, Kogel CA, Soho SK, Gibson JJ, Paulsen KD. Electromagnetic breast imaging: Results of a pilot study in women with abnormal mammograms. Radiology 2007;vol. 243(2):350–359. [PubMed: 17400760]
19. Lazebnik M, McCartney L, Popovic D, Watkins CB, Lindstrom MJ, Harter J, Sewall S, Magliocco A, Booske JH, Okoniewski M, Hagness SC. A large-scale study of the ultrawideband microwave dielectric properties of normal breast tissue obtained from reduction surgeries. Phys. Med. Biol 2007;vol. 52:2637–2656. [PubMed: 17473342]
20. Lazebnik M, Popovic D, McCartney L, Watkins CB, Lindstrom MJ, Harter J, Sewall S, Ogilvie T, Magliocco A, Breslin TM, Temple W, Mew D, Booske JH, Okoniewski M, Hagness SC. A large-scale study of the ultrawideband microwave dielectric properties of normal, benign, and malignant breast tissues obtained from cancer surgeries. Phys. Med. Biol 2007;vol. 52:6093–6115. [PubMed: 17921574]
21. Zhu C, Palmer GM, Breslin T, Harter J, Ramanujam N. Diagnosis of breast cancer using diffuse reflectance spectroscopy: Comparison of a Monte Carlo vs. partial least squares analysis based feature extraction technique. Lasers in Surgery and Medicine 2006;vol. 38:714–724. [PubMed: 16799981]
22. Zhu C, Palmer GM, Breslin TM, Harter J, Ramanujam N. Diagnosis of breast cancer using fluorescence and diffuse reflectance spectroscopy: a Monte Carlo model based approach. J. Biomed. Opt. 2007 accepted.
23. Poplack SP, Paulsen KD, Hartov A, Meaney PM, Pogue BW, Tosteson TD, Grove MR, Soho SK, Wells WA. Electromagnetic breast imaging: Average tissue property values in women with negative clinical flndings. Radiology 2004;vol. 231(2):571–580. [PubMed: 15128998]
24. Popovic D, McCartney L, Beasley C, Lazebnik M, Okoniewski M, Hagness SC, Booske JH. Precision open-ended coaxial probes for in vivo and ex vivo dielectric spectroscopy of biological tissues at microwave frequencies. IEEE Trans. Micr. Theory Tech 2005 May;vol. 53(5)
25. Stuchly SS, Sibbald CL, Anderson JM. A new aperture admittance model for open-ended waveguides. IEEE Trans. Micr. Theory Tech 1994 February;vol. 42(2):192–198.
26. Anderson JM, Sibbald CL, Stuchly SS. Dielectric measurements using a rational function model. IEEE Trans. Micr. Theory Tech 1994 February;vol. 42(2):199–204.
27. Zhu C, Palmer GM, Breslin TM, Xu F, Ramanujam N. The use of a multi-separation flber optic probe for the optical diagnosis of breast cancer. J. Biomed. Opt 2005;vol. 10:024032. [PubMed: 15910105]

28. Palmer GM, Zhu C, Breslin TM, Xu F, Gilchrist KW, Ramanujam N. A Monte Carlo based inverse model for calculating tissue optical properties, Part II: Application to breast cancer diagnosis. Appl. Opt 2006;vol. 45(5):1072–1078. [PubMed: 16512551]
29. Prahl, S. Optical Properties Spectra. 2003. http://omlc.ogi.edu/spectra, Oregon Medical Laser Center, http://omlc.ogi.edu/spectra, Internet resource
30. Bohren, CF.; Huffman, DR. Absorption and Scattering of Light by Small Particles. New York: Wiley; 1983.
31. Hagl DM, Popovic D, Hagness SC, Booske JH, Okoniewski M. Sensing volume of open-ended coaxial probes for dielectric characterization of breast tissue at microwave frequencies. IEEE Trans. Micr. Theory Tech 2003 April;vol. 51(4):1194–1206.
32. Liu Q, Zhu C, Ramanujam N. Experimental validation of Monte Carlo modeling of fluorescence in tissues in the UV-visible spectrum. J. Biomed. Opt 2003;vol. 8:223–236. [PubMed: 12683848]
33. Reinoso RF, Telfer BA, Rowland M. Tissue water content in rats measured by dessication. Journal of Pharmacological and Toxicological Methods 1997;vol. 38:87–92. [PubMed: 9403779]
34. Schepps JL, Foster KR. The UHF and microwave dielectric properties of normal and tumour tissues: variation in dielectric properties with tissue water content. Phys. Med. Biol 1980;vol. 25(6):1149–1159. [PubMed: 7208627]
35. Foster KR, Schepps JL. Dielectric properties of tumor and normal tissues at radio through microwave frequencies. J. Microwave Power 1981;vol. 16:107–119.
36. Gabriel S, Lau RW, Gabriel C. The dielectric properties of biological tissues: III. Parametric models for the dielectric spectrum of tissues. Phys. Med. Biol 1196;vol. 41:2271–2293.
37. Campbell AM, Land DV. Dielectric properties of female human breast tissue measured in vitro at 3.2 GHz. Phys. Med. Biol 1992;vol. 37(1):193–210. [PubMed: 1741424]
38. Peters VG, Wyman DR, Patterson MS, Frank GL. Optical properties of normal and diseased human breast tissues in the visible and near infrared. Phys. Med. Biol 1990;vol. 35(9):1317–1334. [PubMed: 2236211]
39. Durduran T, Choe R, Culver JP, Zubkov L, Holboke MJ, Giammarco J, Chance B, Yodh AG. Bulk optical properties of healthy female breast tissue. Phys. Med. Biol 2002;vol. 47:2847–2861. [PubMed: 12222850]
40. Spinelli L, Torricelli A, Pifferi A, Taroni P, Danesini GM, Cubeddu R. Bulk optical properties and tissue components in the female breast from multiwavelength time-resolved optical mammography. J. Biomed. Opt 2004;vol. 9:1137–1142. [PubMed: 15568933]
41. Thomsen S, Tatman D. Physiological and pathological factors of human breast disease that can influence optical diagnosis. Ann. N.Y. Acad. Sci 1998;vol. 838:171–193. [PubMed: 9511805]
42. Cerussi AE, Jakubowski D, Shah N, Bevilacqua F, Lanning R, Berger AJ, Hsiang D, Butler J, Holcombe RF, Tromberg BJ. Spectroscopy enhances the information content of optical mammography. J. Biomed. Opt 2002;vol. 7:60–71. [PubMed: 11818013]

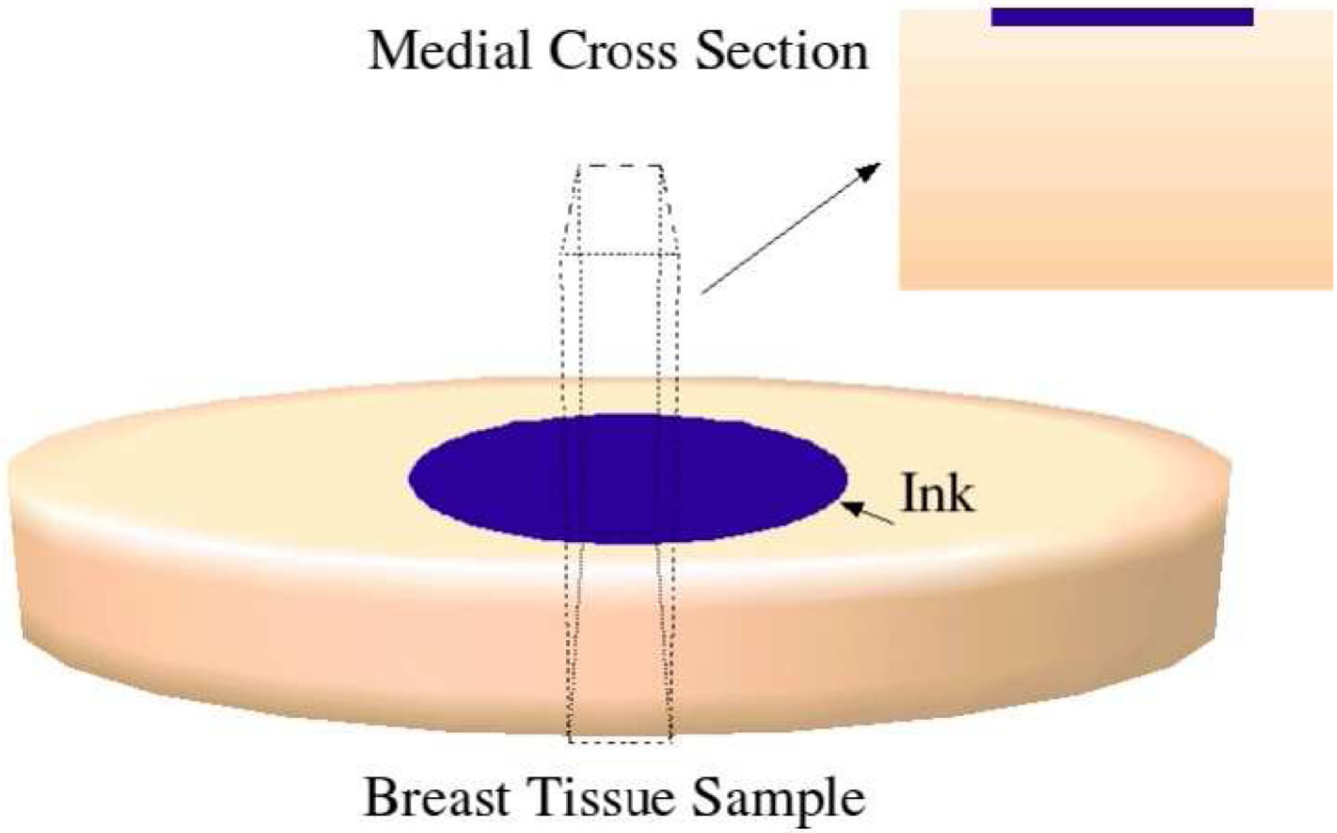

Fig. 1.
Schematic diagram illustrating a medial cross-section through the measurement site, which is processed to create a histology slide.

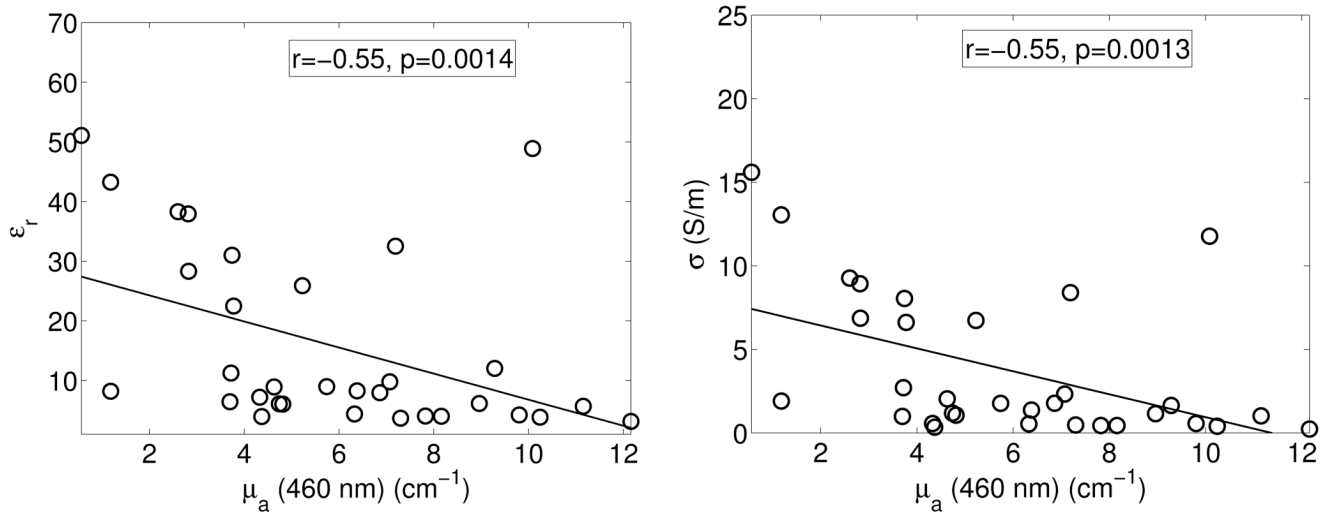

(a) (b)

Fig. 2.

Correlations between the absorption coefficient at 460 nm and (a) dielectric constant at 10 GHz, and (b) effective conductivity at 10 GHz. Symbols: raw data points, solid lines: linear fits through the scatter plots. The boxes show the correlation coefficients and *p*-values for the correlations.

TABLE I

Spearman Correlations between the Dielectric Constant and Effective Conductivity at 5, 10, and 15 GHz and Tissue Composition. Abbreviations: ADIP.: Adipose, GLAND.: Glandular, FIBR. CONN.: Fibroconnective.

	% adip.	% gland.	% fibr. conn.
ε_r (5 GHz)	−0.58	0.55	0.54
σ (5 GHz)	−0.55	0.54	0.52
ε_r (10 GHz)	−0.58	0.55	0.55
σ (10 GHz)	−0.56	0.56	0.53
ε_r (15 GHz)	−0.59	0.55	0.56
σ (15 GHz)	−0.60	0.57	0.57

TABLE II

Spearman Correlations between the Mean Reduced Scattering Coefficients and Absorption Coefficients at 420 nm, 460 nm, 540 nm, and 575 nm, and Tissue Composition. Abbreviations: ADIP.: Adipose, GLAND.: Glandular, FIBR. CONN.: Fibroconnective. (0) No Statistically Significant Correlation.

	% adip.	% gland.	% fibr. conn.
μ_a (420 nm)	0	0	0
μ_a (460 nm)	0.53	−0.59	−0.50
μ_a (540 nm)	0	0	0
μ_a (575 nm)	0	0	0
Mean μ_s'	−0.53	0.42*	0.54

*P<0.02

TABLE III

Spearman Correlations between the Dielectric Constant and Effective Conductivity at 5, 10, and 15 GHz and the Mean Reduced Scattering Coefficient and Absorption Coefficients at 460 nm, 540 nm, and 575 nm. (0) No Statistically Significant Correlation.

	Mean μ_s'		μ_a (460nm)		μ_a(540nm)		μ_a (575nm)	
Freq. (GHz)	ε_r	**σ**	ε_r	**σ**	ε_r	**σ**	ε_r	**σ**
5	0	0	−0.56	−0.55	0	0	0	0
10	0	0	−0.55	−0.55	0	0	0	0
15	0	0	−0.55	−0.53	0	0	0	0